1996

Effects Of Climate Change On Hypoxia In Coastal Waters: A Doubled Co2 Scenario For The Northern Gulf Of Mexico

D Justic

N N. Rabalais

R E. Turner

Recommended Citation

Justic, D., Rabalais, N. N., & Turner, R. E. (1996). Effects Of Climate Change On Hypoxia In Coastal Waters: A Doubled Co2 Scenario For The Northern Gulf Of Mexico. *Limnology And Oceanography, 41* (5), 992-1003. https://doi.org/10.4319/lo.1996.41.5.0992

Limnol. Oceanogr., 41(5), 1996, 992–1003

Effects of climate change on hypoxia in coastal waters: A doubled CO_2 scenario for the northern Gulf of Mexico

Dubravko Justić
Coastal Ecology Institute, Louisiana State University, Baton Rouge 70803

Nancy N. Rabalais
Louisiana Universities Marine Consortium, 8124 Hwy. 56, Chauvin 70344

R. Eugene Turner
Department of Oceanography and Coastal Sciences, Louisiana State University, Baton Rouge 70803

Abstract

Projections of general circulation models suggest that freshwater discharge from the Mississippi River to the coastal ocean will increase 20% if atmospheric CO_2 concentration doubles. This result is likely to affect water column stability, surface productivity, and global oxygen cycling in the northern Gulf of Mexico, which is the site of the largest (up to 16,500 km^2) and most severe hypoxic zone (<2 mg O_2 liter^{-1}) in the western Atlantic Ocean. We use a coupled physical-biological two-box model to investigate potential effects of climate change on seasonal oxygen cycling and hypoxia in river-dominated coastal waters. The model was developed and calibrated using comprehensive environmental data sets collected on the Mississippi River and in the northern Gulf of Mexico between 1985 and 1993. The relative magnitude of changes in river runoff and severity of hypoxia during the 1993 Mississippi River flooding provide an excellent data set for model verification. Model simulations for a doubled CO_2 climate predict a 30–60% decrease in summertime subpycnoclinal oxygen content, relative to a 1985–1992 average. Under those conditions, the hypoxic zone in the northern Gulf of Mexico will expand and encompass an area greater than that of summer 1993.

During this century, the annual mean surface temperatures increased by about 0.5°C on a worldwide basis, with the period 1984–1993 being the warmest decade of the century (Jones et al. 1986, 1988; Kerr 1990; NOAA 1994). Carbon dioxide (CO_2) is considered to be the most important anthropogenic product associated with global warming. CO_2 has been measured continuously at Mauna Loa Observatory, Hawaii, since the late 1950s. This record constitutes the longest CO_2 measurement series in the world and clearly shows steadily increasing concentrations with time (Thorning et al. 1989; NOAA 1994). Although it is still uncertain to what extent global warming during this century can be attributed to increasing atmospheric concentrations of CO_2 and other greenhouse gases (Karl et al. 1991), the trend is apparent, and temperature probably will continue to increase.

Simulations of general circulation models (GCMs), with enhanced greenhouse gas concentrations, provide an estimate for the magnitude of these temperature changes. Giorgi et al. (1994), for example, discussed probable climate scenarios for the continental U.S. using a limited area model (LAM) nested in a GCM. For a doubled CO_2 climate, the experiment produced an average global temperature increase of 3.4°C. Such an increase in global air temperature is likely to affect the global hydrologic cycle. Over oceans, evaporation exceeds precipitation, which is balanced by the runoff of water back to the ocean. For individual river drainage basins, runoff depends on precipitation and evapotranspiration within the basin, as well as on the ability of the ground to store water. Miller and Russell (1992) used a GCM to calculate the annual river runoff for 33 of the world's largest rivers for the present climate and for a doubled CO_2 climate. Model results for a doubled CO_2 climate indicated an increase in runoff for 25 of the 33 rivers. All rivers in high northern latitudes had runoff increases, with a maximum increase of 47%. At low latitudes there were both increases and decreases, ranging from a 96% increase to a 43% decrease. In most cases, the increase in river runoff was coincidental with increased rainfall within the drainage basins (Miller and Russell 1992). Thus, riverine freshwater inputs to the coastal ocean are expected to increase as a result of climate change, at least in some areas.

The northern Gulf of Mexico (Fig. 1), which receives inflows of the Mississippi River, is one of the coastal areas that may experience increased freshwater input in the future. Precipitation in the Mississippi River watershed is likely to increase ~20% with the doubling of atmospheric CO_2 concentration (Miller and Russell 1992;

Acknowledgments

We are grateful to Jay Grymes, who provided the Grand Isle wind data, and to John R. Miller, who provided the Mississippi River discharge data.

This research was funded primarily by a DOE/NIGEC grant. Other sources of support came from NOAA Ocean Assessments Division grants to LUMCON/LSU for hypoxia studies, the NOAA Nutrient Enhanced Coastal Ocean Productivity (NECOP) Program, Louisiana State University, Louisiana Universities Marine Consortium, and the Louisiana Board of Regents LEQSF Program.

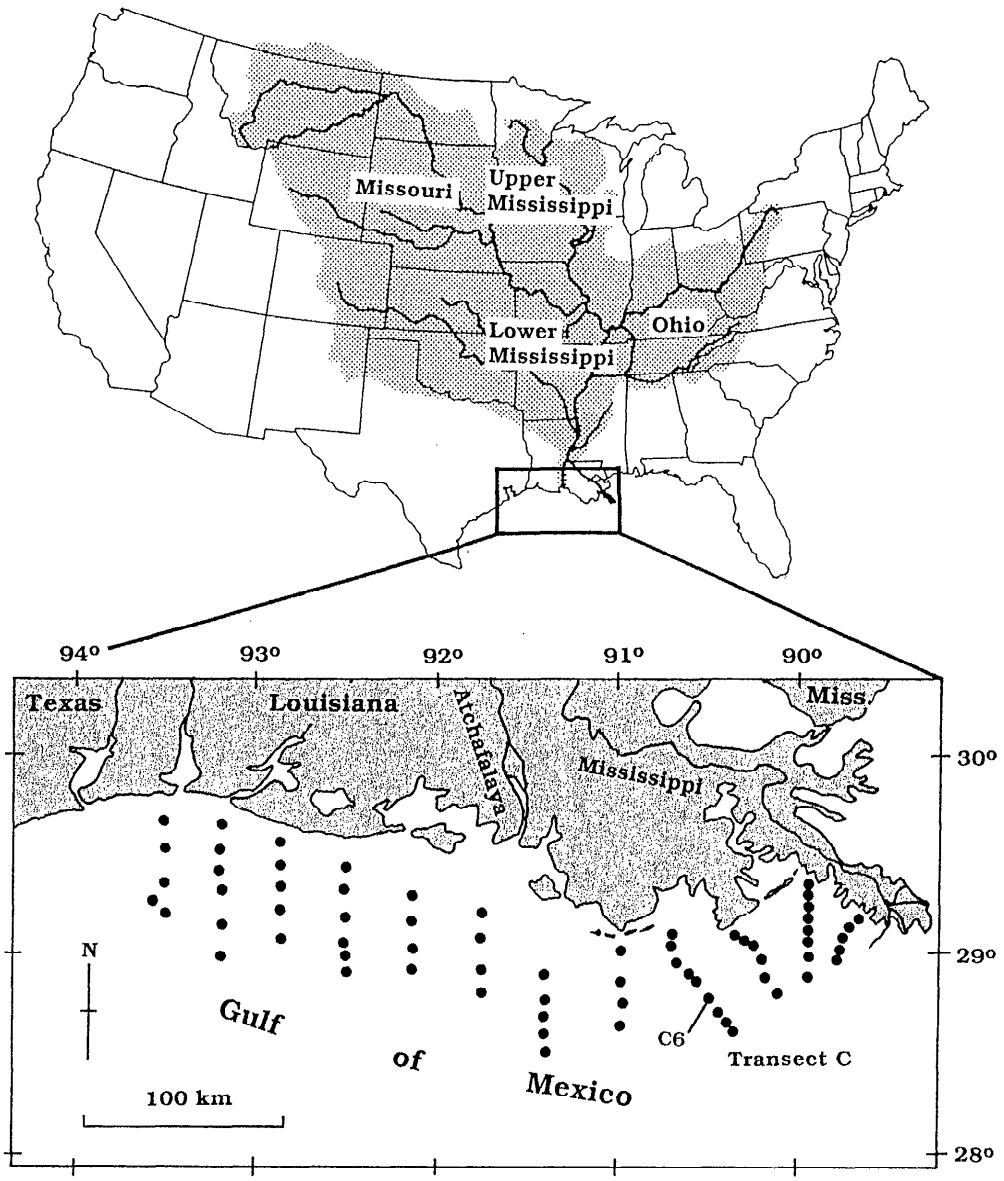

Fig. 1. Map of the drainage basin of the Mississippi River. Station positions are indicated in the lower areal map.

Giorgi et al. 1994). Consequently, Mississippi River runoff is expected to increase in most months, particularly from May through August (Miller and Russell 1992). This result is likely to affect water column stability, surface productivity, and global oxygen cycling in the northern Gulf of Mexico, which is the site of the largest (up to 16,500 km^2) and most severe hypoxic zone in the western Atlantic Ocean (Rabalais et al. 1991, 1994*a*). Hypoxia (<2 mg O_2 liter^{-1}) occurs from April through October in waters below the pycnocline and seems to be causally related to the magnitude and seasonal timing of freshwater and nutrient inputs from the Mississippi River (Justić et al. 1993). During midsummer 1988, for example, hypoxia was minimal in the study area (Fig. 2). Interestingly, 1988 was an extremely dry year during which a 52-yr low discharge record of the Mississippi River was established. In contrast, during the Great Flood of 1993 (a 62-yr maximum discharge for August–September) the areal extent of hypoxia showed a twofold increase with respect to the 1985–1992 average (Fig. 2) (Rabalais et al. 1994*a*). Thus, enhancement of bottom hypoxia seems to be one of the plausible scenarios for climate change in the Gulf Coast region.

Here, we use a two-box oxygen model to investigate the potential effects of climate change on hypoxia in the northern Gulf of Mexico. Our study has three objectives: to provide reliable estimates of global oxygen fluxes across the two main interfaces, air–seawater and pycnocline, for

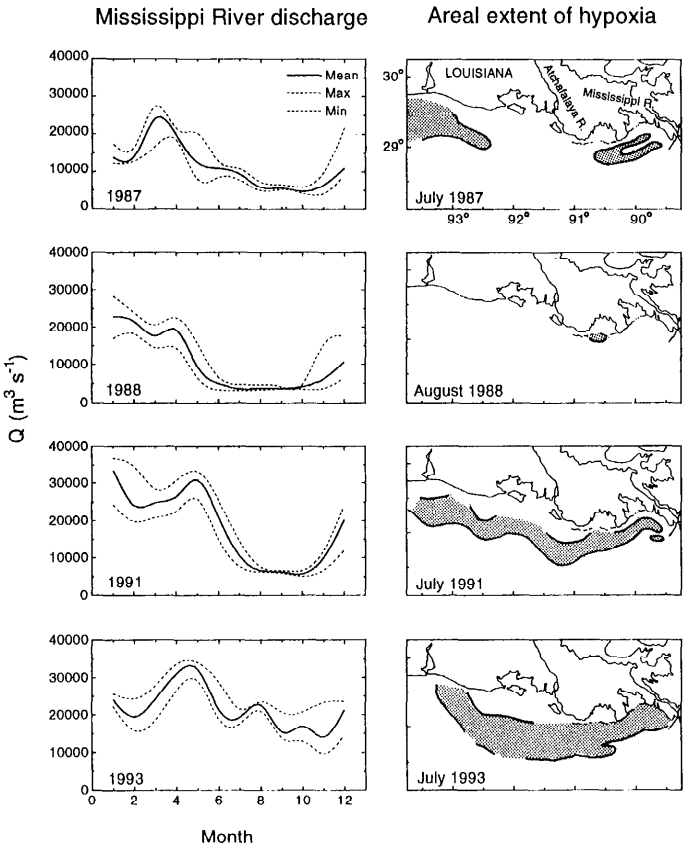

Fig. 2. The Mississippi River discharge (Q) and the areal extent of summer bottom hypoxia in the northern Gulf of Mexico. Shaded areas represent the distribution of bottom waters with dissolved oxygen concentration <2 g O_2 m^{-3} (1.4 ml O_2 $liter^{-1}$).

the present-day climate and for a doubled CO_2 climate; to predict probable changes in seasonal dynamics, severity, and areal extent of hypoxia if CO_2 concentration doubles; and to discuss how such changes may affect animal recruitment, diversity, and overall productivity of a coastal marine ecosystem.

Study area

The northern Gulf of Mexico is strongly influenced by the Mississippi and Atchafalaya Rivers, the discharges of which account for 98% of the total freshwater input (Dinnel and Wiseman 1986). Plumes of the two rivers rapidly form the Louisiana Coastal Current, a highly stratified current that flows, on average, westward along the Louisiana coast and southward along the Texas coast. A strong seasonal pycnocline ($\Delta\sigma_t$ = 4–10 kg m^{-3}), largely due to salinity gradients, persists from April through October (Rabalais et al. 1991). Annual integrated primary productivity is high and ranges from 290 (Sklar and Turner 1981) to 329 g C m^{-2} yr^{-1} (Lohrenz et al. 1990). Due to the shallowness of this region (~20 m, on average), nutrient enhancement of surface primary productivity creates a high carbon flux to the sediments. Rabalais et al. (1991) postulated that ~50% of the primary production reaches the sediments in the northern Gulf of Mexico. This high carbon flux fuels hypoxia in the bottom water below the seasonal pycnocline. Hypoxia is found in 5–60-m water depth, 5–60 km offshore, and extends up to 20 m above the bottom (Rabalais et al. 1991).

Methods

The data on temperature, salinity, and dissolved oxygen were obtained from a series of monitoring cruises conducted during June 1985–October 1993 across the width of the Louisiana shelf, primarily in midsummer. A more frequent sampling program was carried out along transect C on the southeastern shelf (Fig. 1), which was occupied on a biweekly to monthly basis. Station depths ranged from 5 to 30 m. Standard water-column profile data were obtained from either a Hydrolab Surveyor or a SeaBird CTD system with SBE 13-01 (S/N 106) dissolved oxygen meter. The dissolved oxygen measurements were calibrated with Winkler titrations (Parsons et al. 1984) that were periodically carried out during deployment of the instruments.

Continuous temperature and oxygen measurements (15-min intervals) were also obtained at station C6 from July 1990 through October 1992 with an Endeco 1184 pulsed dissolved oxygen sensor. The instrument was deployed ~1 m above the seabed in a 20-m water column. Predeployment and postdeployment calibrations of the pulsed dissolved oxygen sensors were performed in accordance with factory specifications. Continuous oxygen measurements were controlled during hydrographic surveys of the study area, by comparison with Winkler titrations, Hydrolab Surveyor, or SeaBird CTD data.

Daily discharge data (1985–1993) for the Mississippi River at Tarbert Landing were obtained from the U.S. Army Corps of Engineers. Tarbert Landing is in Mississippi, 12.9 km downstream from the inlet channel to the Old River control structure (river mile 306.3). The Old River control structure diverts about a third of the Mississippi River discharge to the Atchafalaya River.

Hourly wind-speed data (1985–1993) for Grand Isle, Louisiana, were obtained from the Louisiana Office of State Climatology.

Theoretical considerations

Approach to modeling—Our basic assumption is that doubling of atmospheric CO_2 will cause major changes in temperature, salinity, net productivity, and oxygen cycling in the northern Gulf of Mexico. The model we seek should provide accurate estimates of oxygen fluxes across the sea surface and the pycnocline over a broad range of temperature and salinity conditions. It should also provide reliable estimates of net oxygen production in the surface layer and total oxygen consumption in the bottom layer. We adopted a two-box model (Fig. 3) by assuming uniform properties for the layers above and below the

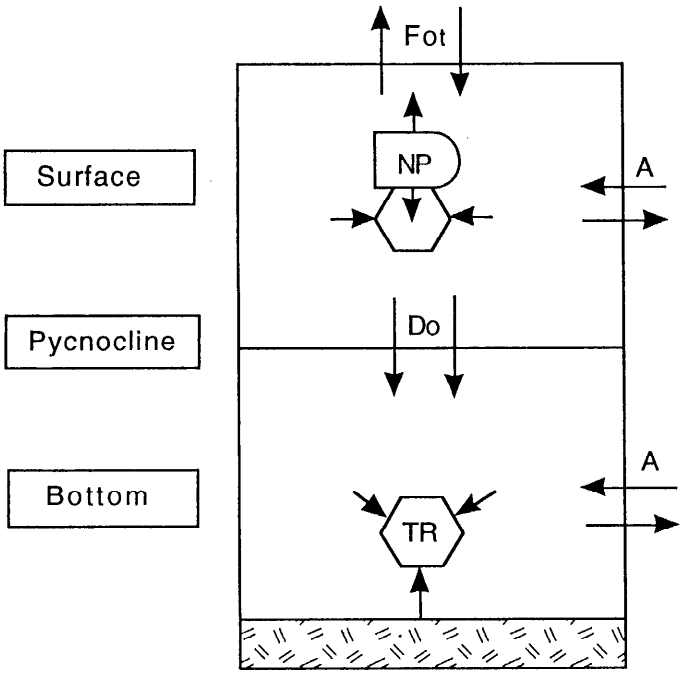

Fig. 3. Conceptual model of oxygen cycling in a shallow, stratified coastal ecosystem. F_{Ot} denotes the total air–sea oxygen flux, NP is the net productivity of the upper layer, D_O the diffusive oxygen flux through the pycnocline, A the horizontal oxygen transport by advection and diffusion, and TR the total oxygen uptake in the lower water column.

Notation

A	Horizontal oxygen transport by advection and diffusion, g O_2 m^{-2} d^{-1}
D_O	Diffusive oxygen flux through the pycnocline, g O_2 m^{-2} d^{-1}
ε	Turbulent kinetic energy dissipation rate, m^{-2} s^{-3}
F_{Ot}	Total air–sea oxygen flux, g O_2 m^{-2} d^{-1}
g	Acceleration due to gravity (=9.81 m s^{-2})
INT_s	Rate of change in the oxygen content of the upper water column, g O_2 m^{-2} d^{-1}
INT_b	Rate of change in the oxygen content of the lower water column, g O_2 m^{-2} d^{-1}
K_z	Vertical eddy diffusivity, m^2 s^{-1}
N	Buoyancy frequency, s^{-1}
NP	Net productivity of the upper water column, g O_2 m^{-2} d^{-1}
O_2	Ambient oxygen concentration, g O_2 m^{-3}
O_2'	Oxygen saturation value, g O_2 m^{-3}
O_s	Average oxygen concentration in the upper water column, g O_2 m^{-3}
O_{ts}	Total oxygen content of the upper water column, g O_2 m^{-2}
O_b	Average oxygen concentration in the lower water column, g O_2 m^{-3}
O_{tb}	Total oxygen content of the lower water column, g O_2 m^{-2}
Q	River runoff, m^3 s^{-1}
ρ	Density, kg m^{-3}
ρ_w	Average density of the water column, kg m^{-3}
$\Delta\rho$	Density gradient between the lower and the upper water column, kg m^{-3}
S	Salinity, psu
T	Temperature, °C
TR	Oxygen uptake rate in the lower water column, g O_2 m^{-2} d^{-1}
V	Transfer velocity, m d^{-1}
W	Wind speed, m s^{-1}
z	Depth, m

average depth of the pycnocline. We chose this approach for the following reasons. The pycnocline in the northern Gulf of Mexico is ~10 m below the surface, in an area where the average depth is 20 m. Thus, during most of the year, the pycnocline divides the water column into two distinct water bodies of about equal volume. In the inner section of the hypoxic zone (sta. C6), vertical oxygen transport is likely to be more important than horizontal oxygen transport. This ranking is suggested by a relatively high coherence between changes in vertical temperature gradients and changes in bottom oxygen concentration (Rabalais et al. 1992). In contrast, a strong tidal signal of any kind, which would indicate horizontal transport, is not present in the periodograms of oxygen data series from station C6 (Rabalais et al. 1994*b*). Also, maximum lateral displacement of only 3 km can be expected due to diurnal and semidiurnal currents (Rabalais et al. 1994*b*), which is not likely to affect the inner section of a 60-km-wide hypoxic zone (Fig. 2).

The oxygen concentration in the upper water column changes as a result of biological oxygen production and consumption, oxygen transport in the horizontal and vertical direction, and atmospheric exchanges (Fig. 3). By neglecting horizontal oxygen transport due to advection and diffusion (A), the oxygen balance in the upper water column (O_s, 0–10-m depth) can be described by the expression

$$dO_s/dt = NP - F_{Ot} - D_O. \quad (1)$$

t is time (d), NP is the net productivity expressed in terms of oxygen equivalents, F_{Ot} is the total air–sea oxygen flux, and D_O is the diffusive oxygen flux through the pycnocline (units given in list of notation). Because of the high turbidity of the continental shelf waters near the Mississippi River, primary productivity is low below a depth of 10 m (Lohrenz et al. 1990) and can be considered insignificant when compared to vertical oxygen transport. Thus, the balance equation for oxygen in the lower water column (O_b, 10–20 m) includes only two terms: oxygen uptake due to benthic and water-column respiration (TR), and oxygen resupply from the upper water column via turbulent diffusion (D_O):

$$dO_b/dt = -TR + D_O. \quad (2)$$

In simulation experiments, the two model equations (Eq. 1 and 2) were integrated over a period of 1 yr using the Runge-Kutta integration method of the fourth order and an integration step of 0.1 d. Computation of individual model terms from Eq. 1 and 2 is discussed below.

Air–sea oxygen flux—Oxygen transport through the sea surface is a result of the difference in the partial pressure of the gas in the surface layer and in the atmosphere. Transfer velocity is thought to be a function of temperature and wind speed. In our calculations we used the formulation proposed by Stigebrandt (1991), which takes into account the effect of gas transfer due to bubbles:

$$F_{Ot} = V(O_2 - 1.025\ O_2'). \quad (3)$$

V is transfer velocity, O_2 is the ambient surface oxygen concentration (0–1 m), and O_2' is the oxygen saturation value. Negative F_{Ot} values indicate that the oxygen flux is directed toward the water column. The transfer velocity was computed from a formula given by Liss and Merlivat (1986):

$$V = 5.9\ Sc^{-0.5}(aW + b). \quad (4)$$

Sc is the Schmidt number, and W is wind speed. Values of constants a and b depend on wind speed. In the interval $3.6 < W < 13$ m s^{-1} these constants are equal to 2.85 and −9.65 (Liss and Merlivat 1986). Schmidt numbers for oxygen can be computed from surface temperature data (T), using a simple analytical expression derived by Stigebrandt (1991):

$$Sc = 1{,}450 - 71\ T + 1.1\ T^2. \quad (5)$$

Oxygen flux through the pycnocline—The vertical diffusive flux of oxygen (D_O) was estimated from

$$D_O = -K_z(\partial O_2/\partial z). \quad (6)$$

K_z is the vertical eddy diffusivity and z is depth. We will assume that the only properties of the stratified water column controlling K_z are the turbulent kinetic energy dissipation rate (ε) and the buoyancy frequency (= Brunt-Väisälä frequency) (N):

$$K_z = a\ \varepsilon\ N^{-2}. \quad (7)$$

Various values for parameter a have been suggested (e.g. Denman and Gargett 1983). Because of the high stability of the water column in the northern Gulf of Mexico (*see Table 2*), we adopted the value of 0.8 (Weinstock 1978). This value is thought to be valid for strong and intermediate stratification, where the Cox number is <2,500 (Caldwell et al. 1980). We assumed that ε at a depth of 10 m is in the range of 10^{-7} m^2 s^{-3}, which is likely to be an upper estimate. Corresponding values were obtained from microstructure measurements in the upper ocean during high winds (Dillon and Caldwell 1980). N was calculated directly from the conductivity-temperature-depth profiles (CTD) using the expression

$$N^2 = (g/\rho_w)(\partial\rho/\partial z). \quad (8)$$

g is the acceleration due to gravity, ρ_w is the average density of the water column, and $\partial\rho/\partial z$ is the vertical density gradient (kg m^{-4}).

Net productivity of the upper water column—Computation of the air–sea oxygen flux (F_{Ot}) and the diffusive oxygen flux through the pycnocline (D_O) enables us to estimate the net oxygen production in the upper water column (0–10 m). From Eq. 1 it follows that

$$NP = INT_S + F_{Ot} + D_O. \quad (9)$$

INT_s is the rate of change in the oxygen content of the upper water column, given as

$$INT_s = \int_0^{10} (dO_2/dt)\ dz. \quad (10)$$

The average INT_s value for a given month (t) may be calculated as an arithmetic mean of changes in the oxygen content with respect to the two adjacent months, $(t - 1)$ and $(t + 1)$:

$$INT_s(t) = \{[O_{ts}(t) - O_{ts}(t - 1)] + [O_{ts}(t + 1) - O_{ts}(t)]\}/2. \quad (11)$$

Here, $O_{ts}(t - 1)$, $O_{ts}(t)$, and $O_{ts}(t + 1)$ are the average oxygen contents of the 0–10-m water column for months $t - 1$, t, and $t + 1$. Moving averages computed from Eq. 11 provided more accurate results in comparison with simple month-to-month differences. The method shown above (Eq. 9–11) is simple because the computation of NP depends only on O_{ts}, F_{Ot}, and D_O.

Oxygen uptake in the lower water column—If the diffusive flux of oxygen through the pycnocline (D_O) is known, we can estimate the total respiration rate in the lower water column (TR). From Eq. 2 it follows

$$TR = -INT_b + D_O \quad (12)$$

where

$$INT_b = \int_{10}^{20} (dO_2/dt)\ dz. \quad (13)$$

As in Eq. 11, the average INT_b value for a given month (t) can be calculated as

$$INT_b(t) = \{[O_{tb}(t) - O_{tb}(t - 1)] + [O_{tb}(t + 1) - O_{tb}(t)]\}/2. \quad (14)$$

O_{tb} is the total oxygen content in the lower water column.

Results

River runoff, salinity, and temperature for a doubled CO_2 climate—Between 1985 and 1992, the average monthly runoff (Q) of the Mississippi River at Tarbert Landing ranged from 6.9×10^3 to 2.4×10^4 m^3 s^{-1} (Fig. 4). The average integrated annual runoff was 0.42×10^{12} m^3. This period includes 2 yr with above-average discharge (1990, 1991), 3 yr with below-average discharge (1987, 1988, 1992), and 3 yr with average discharge (1985, 1986, 1989) and can be considered representative for the present-day climate.

Based on simulations of a GCM, Miller and Russell (1992) predicted that the annual freshwater runoff of the Mississippi River will increase 20% if the concentration of atmospheric CO_2 doubles. A higher runoff is expected

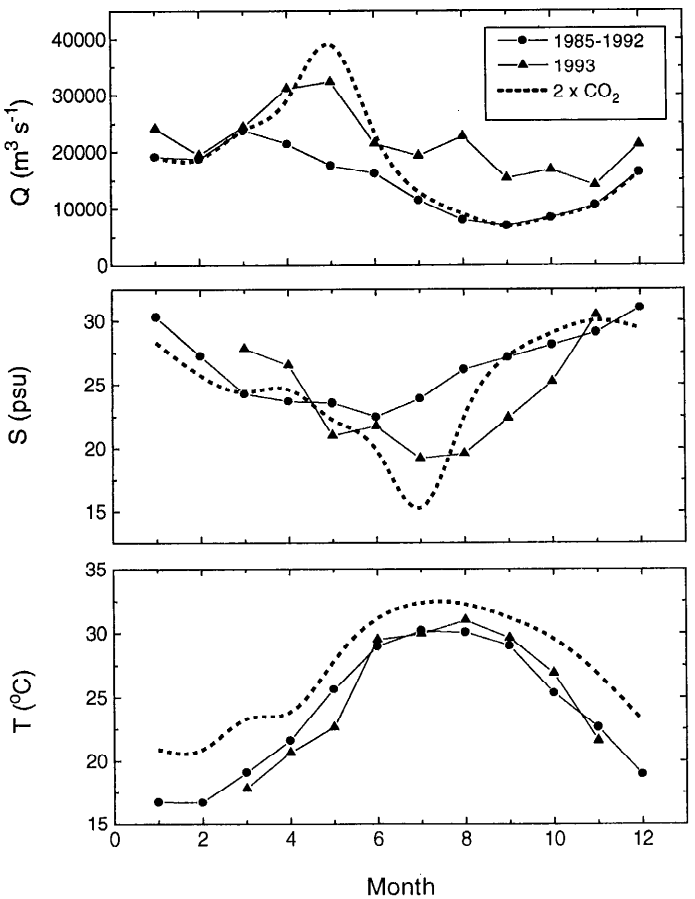

Fig. 4. Observed values of the Mississippi River runoff (Q) at Tarbert Landing, surface salinity (S), and surface temperature (T) at station C6 for 1985–1992 and 1993 and model predictions for a doubled CO_2 climate.

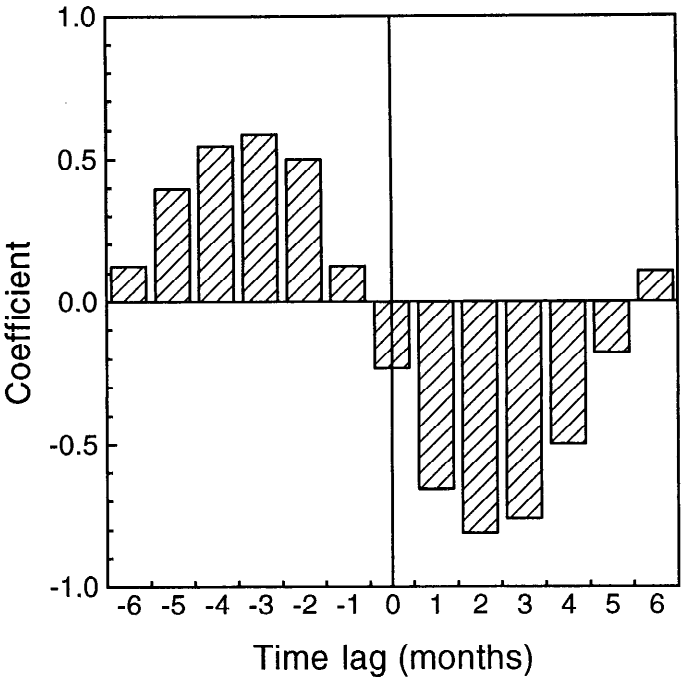

Fig. 5. Cross-correlation function for the Mississippi River water runoff at Tarbert Landing and surface salinity at station C6 for 1985–1992.

primarily during May–August, with runoff peaking in May. We adopted this scenario by using the average Mississippi River runoff for 1985–1992 as a reference for the present-day climate. If the runoff increases 20%, the integrated doubled CO_2 runoff at Tarbert Landing will be $\sim 0.5 \times 10^{12}$ m^3 yr^{-1}. If we assume that the increase in runoff with be highest in May (Miller and Russell 1992), the maximum monthly Q value for a doubled CO_2 climate will be $\sim 4 \times 10^4$ m^3 s^{-1} (Fig. 4). This result is substantially higher than the monthly Q maximum for the Great Flood of 1993 (3.2×10^4 m^3 s^{-1}) (Fig. 4).

Surface salinity on the inner continental shelf of the northern Gulf of Mexico is likely to decrease significantly following a 20% increase in the Mississippi River runoff. This is inferred from a highly significant coherence between the runoff at Tarbert Landing and surface salinity (S) at station C6 (Fig. 5). The cross-correlation coefficient (CCC), computed from monthly Q and S averages for 1985–1992 peaks at the time lag of 2 months (CCC = -0.81; $P < 0.01$). A similar 2-month delay is evident from the Q and S plots for the Great Flood of 1993 (Fig. 4). The best-fit time-delayed linear model is

$$S_t = 33.19 - 0.00046\, Q_{t-2}. \quad (15)$$

This highly significant relationship explains 80% of the variability in surface S values at station C6 during 1985–1992 (Fig. 6); therefore, this relationship should provide reasonable projections of surface salinity for a doubled CO_2 climate. From Eq. 15 and projected doubled CO_2 discharge (Fig. 4), we estimated that midsummer surface salinities at station C6 will be in a 15–20 psu range (Fig. 4). This result is significantly lower (t-test; $P < 0.01$) than the surface S values measured during the Great Flood of 1993 (Fig. 4).

The observed seasonal pattern of surface temperature in the northern Gulf of Mexico closely approximates a cosine curve (Fig. 4). The mean monthly minimum and maximum temperatures for 1985–1992 were 16.7 (February) and 30.2°C (July). With a doubling of atmospheric CO_2 concentration, global air temperature over the Gulf Coast region is expected to increase 4.2°C during winter and 2.2°C during summer (Giorgi et al. 1994). We assume that the increase in air temperature over the Gulf Coast region will be followed by a corresponding increase in sea surface temperature on the inner continental shelf. For station C6, the projected surface minimum and maximum temperatures are 20.9 (February) and 32.4°C (July) (Fig. 4). Importantly, a doubled CO_2 temperature may exceed 30°C throughout the May–October period.

Global oxygen fluxes for present and a doubled CO_2 climate—The oxygen flux through the air–sea interface (F_{Ot}, Eq. 3) is influenced by the surface temperature and

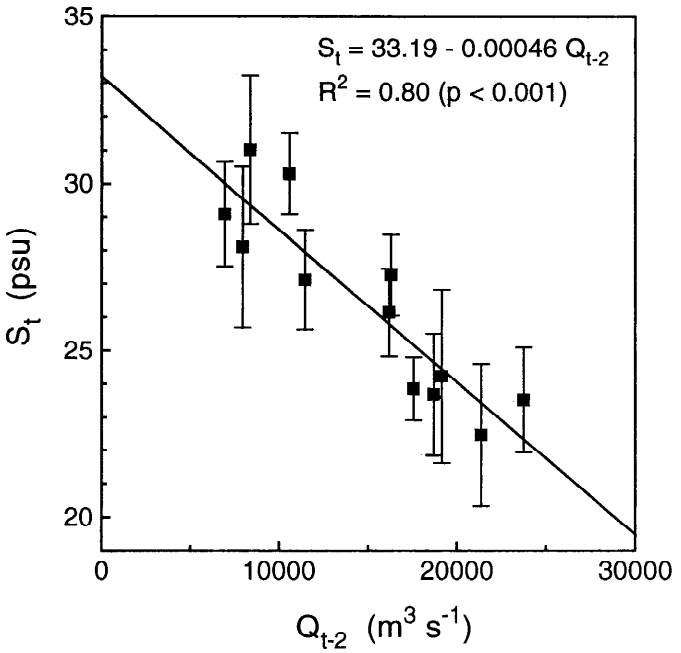

Fig. 6. Relationship between the Mississippi River runoff (Q) at Tarbert Landing and surface salinity (S) at station C6 delayed for 2 months. Symbols represent monthly means and standard errors for 1985–1992.

oxygen departure from O_2 saturation in the surface layer ($O_2 - O_2'$). Using Eq. 3–5 we computed the average monthly F_{Ot} values for station C6 (Table 1). Results for 1985–1992 show that oxygen is released to the atmosphere from February through June. From July through January the surface layer is undersaturated in oxygen and the net flux is directed toward the water column. The calculated F_{Ot} values range from -0.9 to 3.5 g O_2 m^{-2} d^{-1} and seem to be relatively high in comparison with other coastal areas (i.e. Stigebrandt 1991). The integrated net annual F_{Ot} value for station C6 is 226 g O_2 m^{-2} (Table 1).

We expect that the F_{Ot} values will increase with the doubling of atmospheric CO_2 concentration. For a projected doubled CO_2 temperature (Fig. 4), Eq. 4 and 5 predict a 10% increase in transfer velocity (V) during winter and spring (Fig. 7). If the $O_2 - O_2'$ value remains unchanged, the annual net F_{Ot} value will increase from 226 (Table 1) to 240 g O_2 m^{-2}, which is a small change. This is a conservative estimate, however, because the surface oxygen surplus is likely to increase with increasing riverine influence. A linear regression of $O_2 - O_2'$ on S (data from Table 1), for example, reveals that there is a 0.26 g O_2 m^{-3} increase in surface oxygen surplus for a 1 psu decrease in surface salinity ($R = -0.69$; $P < 0.05$). With a doubling of atmospheric CO_2 concentration, surface salinity during the May–August period is expected to decrease by an average of 4 psu (Fig. 4). As a result, we expect an increase in surface oxygen surplus of ~1 g O_2 m^{-3} during those months. This will increase the annual net F_{Ot} value by 39% (from 226 to 314 g O_2 m^{-2} yr^{-1}).

Changes in salinity and temperature of the surface layer will significantly affect the stability of the water column. At station C6, 85% of the variability in the density gradient between the lower and upper water column ($\Delta\rho$) can be explained by a multiple regression on surfacc S and T:

$$\Delta\rho = 17.46 - 0.63\ S + 0.12\ T. \qquad (16)$$

Predicted vs. observed values for 1985–1992 are shown in Fig. 8. From Eq. 16 and S and T projections (Fig. 4) we estimated $\Delta\rho$ values for a doubled CO_2 climate. Results show (Fig. 7) that the $\Delta\rho$ values are likely to exceed 8 kg m^{-3}, during the June–August period. This result is significantly higher (t-test; $P < 0.01$) than the midsummer $\Delta\rho$ average for the Great Flood of 1993 (Fig. 7).

The diffusive oxygen flux through the pycnocline (D_O, Eq. 6–8) is a function of eddy diffusivity (K_z) and vertical gradient in dissolved oxygen concentration. Computational results for station C6 (Table 2) show that K_z de-

Table 1. Average total air-sea oxygen fluxes (F_{Ot}, g O_2 m^{-2} d^{-1}) at station C6 for 1985–1992. Positive F_{Ot} values indicate oxygen loss to the atmosphere. Also shown are monthly averages for the surface layer (0–1 m) of temperature (T, °C), salinity (S, psu), dissolved oxygen concentration (O_2, g O_2 m^{-3}), oxygen saturation value (O_2, g O_2 m^{-3}), wind speed (W, m s^{-1}), and transfer velocity (V, m d^{-1}). Number of observations—n (except for W, which is computed from hourly data). The integrated net annual F_{Ot} value is 226 g O_2 m^{-2}.

	n	T	S	O_2	O_2'	W	V	F_{Ot}
Jan	2	16.72	30.31	7.84	8.11	5.52	1.50	−0.71
Feb	13	16.67	27.27	9.10	8.27	5.56	1.53	0.95
Mar	22	19.09	24.23	9.70	8.03	5.37	1.50	2.20
Apr	22	21.61	23.69	10.12	7.68	5.29	1.55	3.47
May	27	25.64	23.53	9.81	7.15	4.81	1.27	3.16
Jun	34	28.95	22.47	7.79	6.80	4.30	0.86	0.71
Jul	63	30.18	23.86	6.52	6.61	3.69	0.29	−0.07
Aug	30	30.05	26.15	6.45	6.55	3.56	0.17	−0.04
Sep	26	28.98	27.13	6.39	6.63	4.53	1.08	−0.44
Oct	25	25.34	28.11	6.69	7.01	5.13	1.55	−0.77
Nov	8	22.61	29.10	7.47	7.31	5.47	1.74	−0.04
Dec	8	18.93	31.02	7.37	7.74	5.48	1.57	−0.89

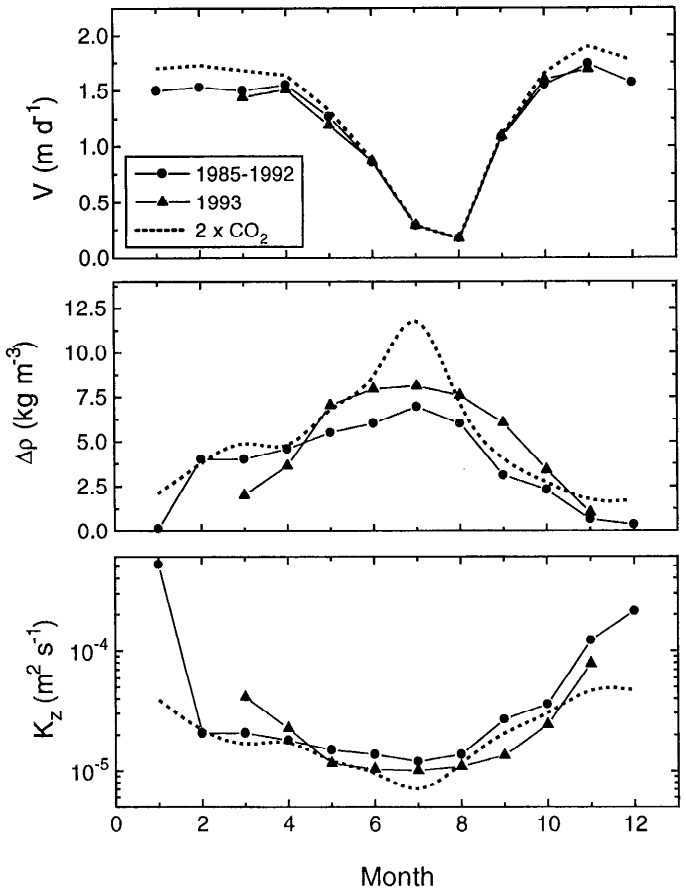

Fig. 7. Computations of transfer velocity (V), water column stability ($\Delta\rho$), and vertical eddy diffusivity (K_z) at station C6 for 1985–1992 and 1993, and model predictions for a doubled CO_2 climate.

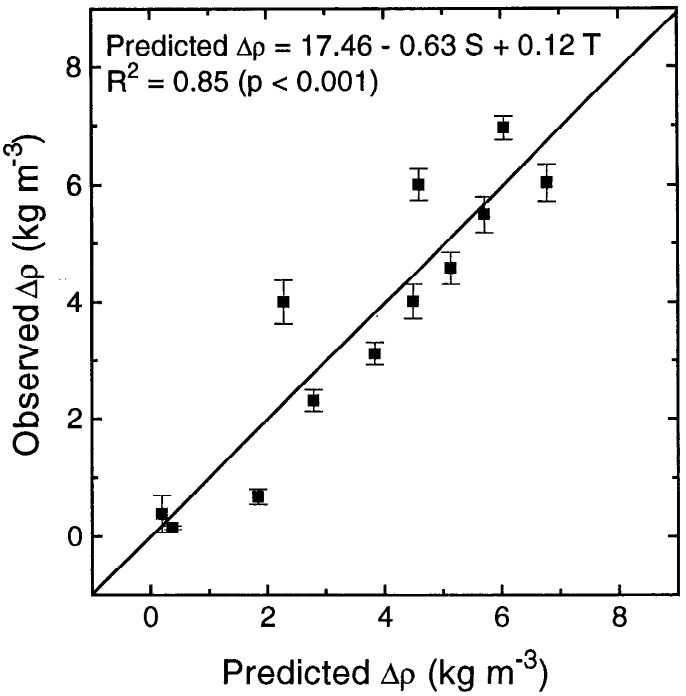

Fig. 8. Observed vs. predicted density gradients between the lower and the upper water column ($\Delta\rho$) at station C6. Symbols represent monthly means and standard errors for 1985–1992.

creases from 5.2×10^{-4} m^2 s^{-1} in January to 1.2×10^{-5} m^2 s^{-1} in July. The D_O values are in the range of 0.2–0.93 g O_2 m^{-2} d^{-1}, which gives an annual integrated oxygen flux of 197 g O_2 m^{-2} (Table 2). From Eq. 7 and 8 it is evident that K_z is inversely related to $\Delta\rho$. As a result of increasing $\Delta\rho$ (Fig. 7), the midsummer K_z values are expected to decrease 25% relative to the 1985–1992 average (Fig. 7). Consequently, if the oxygen gradients between the upper and the lower water column remain unchanged, the integrated D_O value may decrease with a doubling of atmospheric CO_2 concentration, from 197 (Table 2) to 148 g O_2 m^{-2} yr^{-1}. The latter value, however, is a lower estimate. Most likely, vertical oxygen gradients will increase because of increasing oxygen surplus in the upper water column and increasing bottom oxygen deficit, and the integrated D_O value will remain anywhere in the range of 148–197 g O_2 m^{-2} year^{-1}.

Coupling among climate change, surface net productivity, and bottom hypoxia—Computational results for 1985–1992 (Table 3) show that 90% of the annual net oxygen production (NP) at station C6 occurs between February and June. The integrated annual net productivity of the upper water column (0–10 m) at station C6 is 423 g O_2 m^{-2} (Table 3). If a oxygen-to-carbon ratio of 3.47 by weight (mol O_2 : mol C = 138 : 106; PQ = 1.3) is assumed for the photosynthetic process, then the total net carbon production is 122 g C m^{-2} yr^{-1}. This excess of organic matter, derived from primary production, is redistributed within the system, and eventually decomposed in the lower water column and in the sediments. Using Eq. 12–14 we calculated the integrated oxygen uptake rates for the lower water column (TR). Results for station C6 show (Table 4) that the TR values are significantly higher (t-test; $P < 0.01$) between January and June than during the rest of the year. This correlates well with the seasonal changes in NP of the upper water column (Table 3). Formation of the hypoxic bottom waters in the northern Gulf of Mexico, therefore, seems to be associated with the decay of organic matter deposited in the pelagic strata. The integrated annual respiration rate in the lower water column at station C6 is 197 g O_2 m^{-2} yr^{-1} (Table 4). This converts to a value of 57 g C m^{-2} yr^{-1}, if we use an RQ value of 0.77 (mol C : mol O_2 = 106 : 138) for the respiration process. Thus, on an annual basis, 47% of the surface net organic production at station C6 is decomposed in the lower water column and in the sediments (TR : NP = 0.47).

Surface net productivity likely will increase as a result of climate change. This prediction is inferred from a high coherence between the Mississippi River runoff at Tarbert Landing (Q, Fig. 4) and net productivity at station C6 (NP, Table 3). A time delay between the annual Q and NP maxima appears to be on the order of 1 month. Also, there is a significant inverse linear relationship between

Table 2. Average vertical oxygen fluxes (D_O, g O_2 m^{-2} d^{-1}) at 10-m depth (station C6, 1985–1992). Positive D_O values indicate that oxygen flux is directed toward the bottom. Also shown are average density gradients ($\Delta\rho$, kg m^{-3}) between the lower water column and the upper water column, buoyancy frequency (N, s^{-1}), vertical eddy diffusivity (K_z, m^2 s^{-1}) and oxygen concentration in the upper (O_s) and lower (O_b) water column (g O_2 m^{-3}). Number of observations—n. The integrated annual D_O value is 197 g O_2 m^{-2}.

	n	$\Delta\rho$	N	K_z	O_s	O_b	D_O
Jan	6	0.16	1.24×10^{-2}	5.20×10^{-4}	7.13	6.92	0.94
Feb	36	4.01	6.21×10^{-2}	2.07×10^{-5}	8.90	6.35	0.46
Mar	74	4.02	6.22×10^{-2}	2.07×10^{-5}	8.21	4.59	0.65
Apr	74	4.59	6.64×10^{-2}	1.81×10^{-5}	8.48	4.83	0.57
May	89	5.50	7.27×10^{-2}	1.51×10^{-5}	7.93	3.60	0.57
Jun	110	6.04	7.62×10^{-2}	1.38×10^{-5}	6.55	2.94	0.43
Jul	195	6.96	8.18×10^{-2}	1.20×10^{-5}	5.61	1.18	0.39
Aug	103	6.01	7.60×10^{-2}	1.38×10^{-5}	5.50	1.41	0.49
Sep	89	3.12	5.48×10^{-2}	2.67×10^{-5}	6.39	3.94	0.56
Oct	87	2.31	4.71×10^{-2}	3.60×10^{-5}	6.43	4.76	0.52
Nov	27	0.68	2.56×10^{-2}	1.22×10^{-4}	7.14	6.40	0.78
Dec	23	0.39	1.94×10^{-2}	2.13×10^{-4}	7.50	7.39	0.20

NP and surface salinity. A linear regression of monthly NP averages (Table 3) on S (Table 1) reveals that there is a 9.2 g O_2 m^{-2} $month^{-1}$ increase in NP for a 1 psu decrease in S ($R = -0.60$; $P < 0.05$). With a doubling of atmospheric CO_2, surface salinity during the May–August period is expected to decrease by an average of 4 psu (Fig. 4). As a result, we expect an increase in NP of 37 g O_2 m^{-2} $month^{-1}$ for those months, which will increase the integrated annual NP value by ~35%, from 423 (Table 3) to 571 g O_2 m^{-2} yr^{-1}. This estimate compares well to our calculated 39% increase in annual air–sea oxygen flux. If we assume that the NP : TR ratio will remain at its present value of 0.47, the integrated annual TR value will increase from 197 (Table 4) to 268 g O_2 m^{-2} yr^{-1}.

Subpycnoclinal oxygen content and climate change—Model results suggest that the subpycnoclinal oxygen content at station C6 (O_{tb}) will decrease as a result of climate change. Two different model projections for a doubled CO_2 climate are given in Fig. 9. On the assumption that the NP values and the TR : NP ratio will be the same as those calculated for 1985–1992 (Table 3; TR : NP = 0.47), the O_{tb} values will decrease by ~7 g O_2 m^{-2} between June and September. This is a 30% decrease when compared to the average monthly O_{tb} values for 1985–1992 (Fig. 9). An increase in NP values of 35% during May–August, however, may result in a 60% decrease in summer O_{tb} values (Fig. 9). This could cause the total depletion of oxygen in the water column below the pycnocline, which may persist over a period of several weeks.

Table 3. Seasonal changes in net productivity (NP) of the upper water column at station C6 for 1985–1992. Also shown are total oxygen content of the upper water column (O_{ts}, g O_2 m^{-2}), total air–sea oxygen flux (F_{Ot}), vertical diffusive oxygen flux (D_O), and changes in O_{ts} between successive months (INT_s), all in g O_2 m^{-2} $month^{-1}$.

	O_{ts}	F_{Ot}	D_O	INT_s	NP
Jan	71.30	−21.30	28.20	7.00	13.90
Feb	89.00	28.50	13.80	5.40	47.70
Mar	82.10	66.00	19.50	−2.10	83.40
Apr	84.80	104.10	17.10	−1.40	119.80
May	79.30	94.80	17.10	−9.65	102.25
Jun	65.50	21.30	12.90	−11.60	22.60
Jul	56.10	−2.10	11.70	−5.25	4.35
Aug	55.00	−1.20	14.70	3.90	17.40
Sep	63.90	−13.20	16.80	4.65	8.25
Oct	64.30	−23.10	15.60	3.75	−3.75
Nov	71.40	−1.20	23.40	5.35	27.55
Dec	75.00	−26.70	6.00	−0.05	−20.75
Σ		225.90	196.80	0.00	422.70

Table 4. Seasonal changes in oxygen uptake in the lower water column (TR, g O_2 m^{-2} $month^{-1}$) at station C6 for 1985–1992. Also shown are total oxygen content of the lower water column (O_{tb}, g O_2 m^{-2}), vertical diffusive oxygen flux (D_O, g O_2 m^{-2} $month^{-1}$), and changes in O_{tb} between successive months (INT_b, g O_2 m^{-2} $month^{-1}$).

	O_{tb}	D_O	INT_b	TR
Jan	69.20	28.20	−5.20	33.40
Feb	63.50	13.80	−11.65	25.45
Mar	45.90	19.50	−7.60	27.10
Apr	48.30	17.10	−4.95	22.05
May	36.00	17.10	−9.45	26.55
Jun	29.40	12.90	−8.95	21.85
Jul	18.10	11.70	−7.65	19.35
Aug	14.10	14.70	10.65	4.05
Sep	39.40	16.80	16.75	0.05
Oct	47.60	15.60	12.30	3.30
Nov	64.00	23.40	13.15	10.25
Dec	73.90	6.00	2.60	3.40
Σ		196.80	0.00	196.80

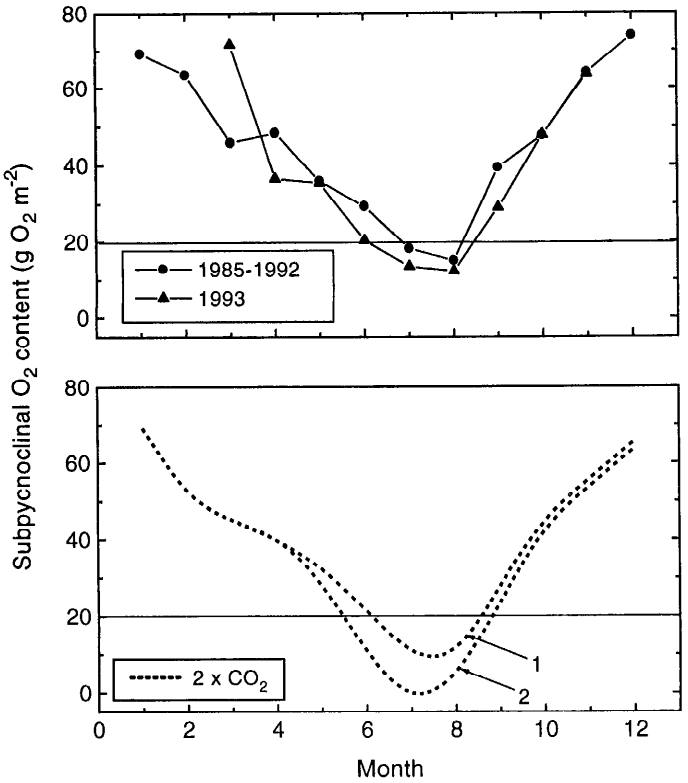

Fig. 9. Seasonal changes in the oxygen content of the lower water column (O_{tb}) during 1985–1992 and 1993 and model predictions for a doubled CO_2 climate. Two model predictions for O_{tb} are shown: 1—integrated NP remains the same as during 1985–1992 (Table 3); 2—the NP value for the May–August period is increased by 35%.

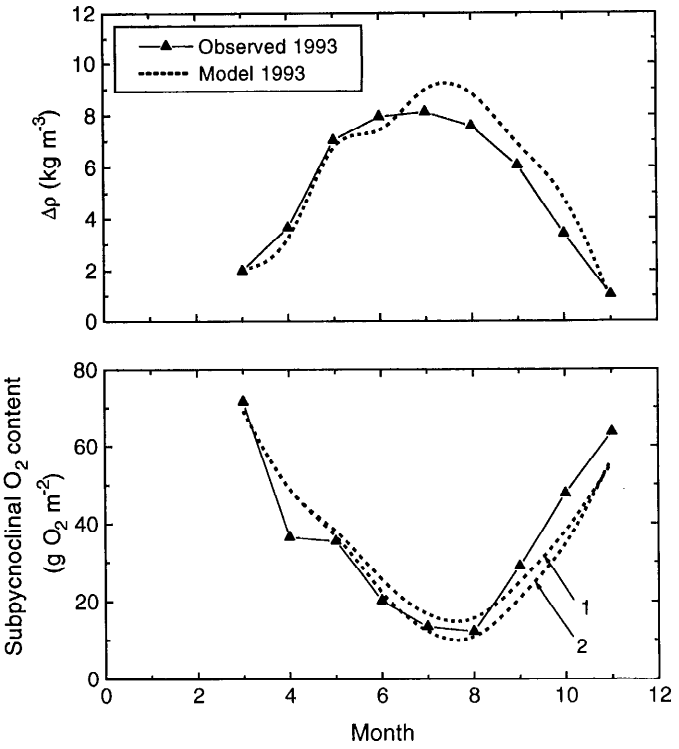

Fig. 10. Observed and predicted 1993 vertical density gradients ($\Delta\rho$) and oxygen content of the lower water column (O_{tb}). Two model projections for O_{tb} are shown: 1—integrated NP remains the same as during 1985–1992 (Table 3); 2—the NP value for the May–August period is increased by 10%.

Discussion

Model verification: Lessons from the 1993 Mississippi River flooding—The flood of 1993 sent large volumes of freshwater down the Mississippi River during a time of year usually characterized by lower flows (Fig. 2). The river flow was above the 62-yr maximum daily record for 37 consecutive days, from 5 August through 10 September (Boyles and Humphries 1994). The higher streamflow of the Mississippi and Atchafalaya Rivers resulted in lower than normal surface salinities, higher surface temperatures, and increased stability in the coastal waters of the northern Gulf of Mexico (Figs. 4, 7). Upstream flooding greatly increased the overall loading of nutrients (Goolsby 1994). Under those nutrient-favorable conditions, the total phytoplankton counts were more than an order of magnitude higher than normal (Dortch 1994). As a result of increased water-column stability and increased vertical carbon flux, the oxygen content of the lower water column was significantly lower (*t*-test; $P < 0.01$) when compared with values from 1985–1992 (Fig. 9). Also, the areal extent of hypoxia showed an approximately twofold increase with respect to the 1985–1992 midsummer average (Rabalais et al. 1994*a*) (Fig. 2).

The Great Flood of 1993 provided an excellent opportunity for verifying our model by running it using the 1993 temperature and salinity data. Initially, we assumed that the values of NP and TR during 1993 were the same as those calculated for 1985–1992 (Tables 3, 4), and thus we examined only the effect of increased stability of the water column on bottom oxygen concentration. This model simulation produced results that agree reasonably well with measured values (Fig. 10). The projected oxygen content during spring and summer, however, is slightly higher than observed, suggesting that TR values were higher in 1993, which we attribute to increased NP in the upper water column. Indeed, in simulation experiments, a 10% increase in NP values for the May–August period, relative to 1985–1992 data, resulted in better agreement between model results and measured values (Fig. 10).

Perspectives for coastal bottom hypoxia in a warmer world—We cannot predict future changes in the areal extent of hypoxia in the northern Gulf of Mexico based on simulations of a two-box model. We hypothesize, however, that if the concentration of atmospheric CO_2 doubles, the zone of hypoxia will expand and encompass an area greater than that of summer 1993 (Fig. 1). Several arguments support this hypothesis. The projected peak runoff of the Mississippi River for a doubled CO_2 climate is substantially higher than the maximal runoff during the Great Flood of 1993 (Fig. 4). Because of increased fresh-

water discharge (Fig. 4) and increased water-column stability (Fig. 7), low-saline and nutrient-rich surface waters of riverine origin will be distributed farther away from the Mississippi River delta. Under those conditions, the surface net productivity and the vertical flux of organic matter are likely to increase. The projected midsummer $\Delta\rho$ values for a doubled CO_2 climate are significantly higher (t-test; $P < 0.01$) when compared to the 1985–1992 and 1993 averages (Fig. 7). Consequently, diffusive oxygen transport between the upper and the lower water column is expected to decrease. Our model suggests that the subpycnoclinal oxygen content on the middle continental shelf may decrease significantly (t-test; $P < 0.01$) below the 1993 minimum if the concentration of atmospheric CO_2 doubles (Fig. 9). This decrease in the bottom oxygen content in the core of hypoxic zone is likely to create a higher oxygen demand in the adjacent bottom waters. As a result, horizontal oxygen transport due to tidal currents will be less effective, and the zone of hypoxia may expand.

We believe NP will increase as a result of climate change. This is because the concentration of primary nutrients—silicon (Si), nitrogen (N), and phosphorus (P)—in the Mississippi River are at least one order of magnitude higher than those in the adjacent coastal waters (Turner and Rabalais 1991; Justić et al. 1995*a*). The increasing riverine freshwater input to the coastal ocean is likely to increase the nutrient levels and thus enhance the growth of phytoplankton. Incidentally, our recent study (Justić et al. 1995*b*) suggests that the stoichiometric ratios of dissolved Si, N, and P in the river are in perfect coincidence with the Redfield ratio (Si : N : P = 16 : 16 : 1), which is a suitable nutrient composition for growth of diatoms and other coastal phytoplankton (Brzezinski 1985; Hecky and Kilham 1988). Thus, as a result of climate change, the Si : N : P ratios in the river-dominated coastal waters may become more balanced and potentially less limiting for phytoplankton growth. Finally, the data for the Great Flood of 1993 also support the hypothesis that NP will increase with increasing riverine influence. The departures from oxygen saturation in the surface layer ($O_2 - O_2'$) during 1993, for example, were significantly higher (t-test; $P < 0.05$) than the average values for 1985–1992.

Consequences for coastal ecosystems—Negative effects of hypoxia have been reported from various coastal and estuarine areas, ranging from mass mortalities of benthic organisms (Stachowitsch 1984; Rosenberg 1985; Boesch and Rabalais 1991) to species extinction (Officer et al. 1984; Benović et al. 1987; Justić 1991). Studies from the northern Gulf of Mexico have shown that species abundance and diversity are drastically reduced when the bottom dissolved oxygen concentration falls below 2 g O_2 m^{-3} (Pavella et al. 1983; Renaud 1986). Furthermore, as the dissolved oxygen levels plummet below 0.5 g O_2 m^{-3}, heavy mortalities occur in the benthic infauna (Gaston 1985; Boesch and Rabalais 1991). As a result, the overall structure of the benthic community in the hypoxic zone shifts toward a polychaete-dominated fauna of smaller individuals and lower standing stock. Presently, the benthic community recovers in fall and has further recruitment in the subsequent spring. If hypoxia worsens, however, due either to increase in duration or severity (Fig. 9), recovery rates may decrease. An increasing incidence of mass mortalities in the benthic infauna will reduce food resources for the recolonizing demersal groups, such as the commercially important penaeid shrimps. Further, motile fish and invertebrates that now migrate from the hypoxic area may be fatally trapped against the shore by a large anoxic water mass. Thus, climate change in the Gulf Coast region likely will have major impacts on benthic and epibenthic species diversity and community structure. This, in turn, will have implications for sedimentary processes, benthic-pelagic coupling, and energy flow.

References

BENOVIĆ, A., D. JUSTIĆ, AND A. BENDER. 1987. Enigmatic changes in the hydromedusan fauna of the northern Adriatic Sea. Nature **326**: 597–600.

BOESCH, D. F., AND N. N. RABALAIS. 1991. Effects of hypoxia on continental shelf benthos: Comparison between the New York Bight and the northern Gulf of Mexico, p. 27–34. *In* R. V. Tyson and T. H. Pearson [eds.], Modern and ancient continental shelf anoxia. Geol. Soc. Spec. Publ. 58.

BOYLES, R., JR., AND R. G. HUMPHRIES. 1994. Lower Mississippi River streamflow, p. 28–29. *In* Coastal oceanographic effects of summer 1993 Mississippi River flooding. NOAA Spec. Rep. NOAA Coastal Ocean Office/Natl. Weather Serv.

BRZEZINSKI, M. A. 1985. The Si : C : N ratio of marine diatoms: Interspecific variability and the effects of some environmental variables. J. Phycol. **21**: 347–357.

CALDWELL, D. R., T. M. DILLON, J. M. BRUBAKER, P. A. NEWBERGER, AND C. A. PAULSON. 1980. The scaling of vertical temperature gradient spectra. J. Geophys. Res. **85**: 1917–1924.

DENMAN, K. L., AND A. E. GARGETT. 1983. Time and space scales of vertical mixing and advection of phytoplankton in the upper ocean. Limnol. Oceanogr. **28**: 801–815.

DILLON, T. M., AND D. R. CALDWELL. 1980. The Batchelor spectrum and dissipation in the upper ocean. J. Geophys. Res. **85**: 1910–1916.

DINNEL, S., AND W. J. WISEMAN, JR. 1986. Freshwater on the Louisiana shelf. Cont. Shelf Res. **6**: 765–784.

DORTCH, Q. 1994. Changes in phytoplankton number and species composition, p. 46–49. *In* Coastal oceanographic effects of summer 1993 Mississippi River flooding. NOAA Spec. Rep. NOAA Coastal Ocean Office/Natl. Weather Serv.

GASTON, G. R. 1985. Effects of hypoxia on macrobenthos of the inner shelf off Cameron, Louisiana. Estuarine Coastal Shelf Sci. **20**: 603–613.

GIORGI, F., C. SHIELDS-BRODEUR, AND G. T. BATES. 1994. Regional climate change scenarios produced with a nested regional climate model. J. Clim. **7**: 375–399.

GOOLSBY, D. A. 1994. Flux of herbicides and nitrate from the Mississippi River to the Gulf of Mexico, p. 32–35. *In* Coastal oceanographic effects of summer 1993 Mississippi River flooding. NOAA Spec. Rep. NOAA Coastal Ocean Office/Natl. Weather Serv.

HECKY, R. E., AND P. KILHAM. 1988. Nutrient limitation of phytoplankton in freshwater and marine environments; a review of recent evidence on the effects of enrichment. Limnol. Oceanogr. **33**: 796–822.

JONES, P. D., AND OTHERS. 1988. Evidence for global warming in the past decade. Nature **332:** 790.

———, T. M. L. WIGLEY, AND P. B. WRIGHT. 1986. Global temperature variation between 1961 and 1984. Nature **322:** 430–434.

JUSTIĆ, D. 1991. Hypoxic conditions in the northern Adriatic Sea: Historical development and ecological significance, p. 95–105. *In* R. V. Tyson and T. H. Pearson [eds.], Modern and ancient continental shelf anoxia. Geol. Soc. Spec. Publ. 58.

———, N. N. RABALAIS, AND R. E. TURNER. 1995*a*. Stoichiometric nutrient balance and origin of coastal eutrophication. Mar. Pollut. Bull. **30:** 41–46.

———, ———, ———, AND Q. DORTCH. 1995*b*. Changes in nutrient structure of river-dominated coastal waters: Stoichiometric nutrient balance and its consequences. Estuarine Coastal Shelf Sci. **40:** 339–356.

———, ———, ———, AND W. J. WISEMAN, JR. 1993. Seasonal coupling between riverborne nutrients, net productivity and hypoxia. Mar. Pollut. Bull. **26:** 184–189.

KARL, T. R., R. R. HEIM, JR., AND R. G. QUAYLE. 1991. The greenhouse effect in North America: If not now, when? Science **251:** 1058–1061.

KERR, R. A. 1990. Global warming continues in 1989. Science **247:** 521.

LISS, P. S., AND L. MERLIVAT. 1986. Air-sea gas exchange rates: Introduction and synthesis, p. 113–127. *In* P. Buat-Ménard [ed.], The role of air-sea exchange in geochemical cycling. Reidel.

LOHRENZ, S. E., M. J. DAGG, AND T. E. WHITLEDGE. 1990. Enhanced primary production in the plume/oceanic interface of the Mississippi River. Cont. Shelf Res. **10:** 639–664.

MILLER, J. R., AND G. L. RUSSELL. 1992. The impact of global warming on river runoff. J. Geophys. Res. **97:** 2757–2764.

NOAA. 1994. Fifth annual climate assessment 1993. Clim. Anal. Center.

OFFICER, C. C., AND OTHERS. 1984. Chesapeake Bay anoxia: Origin, development and significance. Science **223:** 22–27.

PARSONS, T. R., Y. MAITA, AND M. LALLI. 1984. A manual of chemical and biological methods for seawater analyses. Pergamon.

PAVELLA, J. S., J. L. ROSS, AND M. E. CHITTENDEN, JR. 1983. Sharp reduction in abundance of fishes and benthic macroinvertebrates in the Gulf of Mexico off Texas associated with hypoxia. NE Gulf Sci. **6:** 167–173.

RABALAIS, N. N., R. E. TURNER, AND W. J. WISEMAN, JR. 1992. Distribution and characteristics of hypoxia on the Louisiana shelf in 1990 and 1991, p. 15–20. *In* Proc. Nutrient Enhanced Coastal Ocean Productivity Workshop. NOAA Coastal Ocean Program Publ. TAMU-SG-92-109.

———, ———, AND ———. 1994*a*. Hypoxic conditions in bottom waters of the Louisiana–Texas shelf, p. 50–54. *In* Coastal oceanographic effects of summer 1993 Mississippi River flooding. NOAA Spec. Rep. NOAA Coastal Ocean Office/Natl. Weather Serv.

———, ———, ———, AND D. F. BOESCH. 1991. A brief summary of hypoxia on the northern Gulf of Mexico continental shelf: 1985–1988, p. 35–47. *In* R. V. Tyson and T. H. Pearson [eds.], Modern and ancient continental shelf anoxia. Geol. Soc. Spec. Publ. 58.

———, W. J. WISEMAN, JR., AND R. E. TURNER. 1994*b*. Comparison of continuous records of near-bottom dissolved oxygen from the hypoxia zone along the Louisiana coast. Estuaries **17:** 850–861.

RENAUD, M. L. 1986. Hypoxia in Louisiana coastal waters during 1983: Implications for fisheries. Fish. Bull. **84:** 19–26.

ROSENBERG, R. 1985. Eutrophication—the future marine coastal nuisance? Mar. Pollut. Bull. **16:** 227–231.

SKLAR, F. H., AND R. E. TURNER. 1981. Characteristics of phytoplankton production off Barataria Bay in an area influenced by the Mississippi River. Contrib. Mar. Sci. **24:** 93–106.

STACHOWITSCH, M. 1984. Mass mortality in the Gulf of Trieste: The course of community destruction. Mar. Ecol. **5:** 243–264.

STIGEBRANDT, A. 1991. Computation of oxygen fluxes through the sea surface and net production of organic matter with application to the Baltic and adjacent seas. Limnol. Oceanogr. **36:** 444–454.

THORNING, K. W., P. P. TANS, AND W. D. KOMHYR. 1989. Atmospheric carbon dioxide at Mauna Loa Observatory. 2. Analysis of the NOAA/GMCC data, 1974–1985. J. Geophys. Res. **94:** 8549–8565.

TURNER, R. E., AND N. N. RABALAIS. 1991. Changes in the Mississippi River water quality this century—implications for coastal food webs. BioScience **41:** 140–147.

WEINSTOCK, J. 1978. Vertical turbulent diffusion in a stably stratified fluid. J. Atmos. Sci. **35:** 1022–1027.